On Xylographic Image Reconstruction: the Segmentation Phase

Ivan Gerace(✉)

Laboratorio di Matematica Computazionale Sauro Tulipani, Dipartimento di Matematica e Informatica, Università degli Studi di Perugia, Perugia, Italy
ivan.gerace@unipg.it

Abstract. This paper addresses the reconstruction of images from xenographic documents, which often exhibit multiple and varied types of distortions. To effectively resolve these issues, a multi-stage reconstruction process is required, with each stage targeting a specific distortion. A primary challenge in this process is the segmentation of pixels according to the printer's color palette. This study proposes incorporating the segmentation phase at an early stage of reconstruction and introduces a technique to achieve this objective. The experimental results demonstrate promising outcomes for facilitating subsequent reconstruction stages.

Keywords: image reconstruction · image segmentation · color spaces · document reconstruction

Introduction

Since the 14th century, card games have become widespread in Europe, leading to the emergence of various types of local playing cards [15,16,18]. While many of these card types remain in use, others have disappeared. In certain instances, only historical decks produced using xylographic printing techniques and subsequently deteriorated over time have survived. The *Perugine* type is one such example.

A multi-stage technique for the digital reconstruction of such decks was proposed in [13]. The present work revisits and modifies this technique by introducing an additional stage: segmentation [12,22]. Detailed analysis of the reconstruction of xylographic images reveals that the core challenge lies in segmenting pixels according to the limited hues available to historical printers. Following a defading stage [1,9,19,20] that restores the chromatic components of the image to their original saturation, segmentation becomes a crucial step. The segmented image subsequently facilitates the reconstruction of borders and colored regions. Accordingly, a chromatic segmentation technique is proposed that utilizes a uniform color space [4], such as QTLC-r^*g^* (Quadratically Transformed Luminance Chrominance-r^*g^*). This color space is defined by a polynomial transformation from RGB coordinates (see [6]). Employing a uniform color space minimizes discrepancies in visual error during evaluation.

© The Author(s), under exclusive license to Springer Nature Switzerland AG 2027
O. Gervasi et al. (Eds.): ICCSA 2026 Workshops, LNCS 16763, pp. 77–94, 2027.
https://doi.org/10.1007/978-3-032-30530-5_5

The structure of this paper is as follows. Section 1 reviews the printing systems used to produce playing cards. Section 2 discusses the significance of the *Perugine* deck for reconstruction efforts. Section 3 examines the direct problem of producing historical playing cards using xylographic techniques. Section 4 presents the technique proposed in [13] for reconstructing xylographic images. Section 5 introduces the proposed technique for the new segmentation phase, and Sect. 6 presents the experimental results associated with this approach.

1 Printing Systems

Printing techniques for playing cards have varied significantly since their inception. Decks intended for the lower classes were mass-produced using matrices engraved on wooden boards, whereas tarot cards used in courts were hand-painted by renowned artists. Printing systems remained artisanal until the early nineteenth century, when technological advances enabled mass production. The following subsection briefly introduces the most commonly used printing methods [2,5].

1.1 Xylography

The first printing technique used for producing playing cards was *woodcut* or *xylography*. This method uses wooden blocks carved with chisels. The resulting lines are quite bold and clear. The design is created by the protruding part of the block, and the ink is applied to this relief. The inks, both the black for the base design and those for coloring the image, were made by dissolving dye powders in water, along with substances that thickened the color and fixed it to the paper. The colors, initially applied by hand, began to be applied using stencils, with shapes corresponding to the areas to be colored. Woodcut remained in use, at least for the less expensive cards, until the early 20th century. Unfortunately, woodcuts are characterized by often broken lines, as the wooden block has poor resistance to both weathering and wear. Colors are added with stamps or stencils, so in some places their deviation from the black lines and the colored areas that need to be filled in are noticeable. Figure 1 illustrates a wooden block utilized in this printing technique.

1.2 Chalcography

A technique called *chalcography* uses metal plates, rather than wooden ones. This technique began to be used for printing playing cards in the 17th century. Specifically, the metal plate was engraved with a burin, and ink was deposited in the resulting cavity. This technique allowed for finer lines than with woodcuts, thus achieving more realistic shading. Because the ink was in the plate's cavity, to achieve a perfect print, the pressure between the plate and the paper had to be greater than in woodcuts. This resulted in numerous raised areas on the newly printed sheet, making stencil coloring more difficult. Therefore, the paper was often colored with watercolors.



Fig. 1. wooden block for printing *Siciliani* Tarot cards.

1.3 Lithography

Toward the end of the 19th century, a printing method called *lithography* was developed. It involved using a well-polished limestone plate on which the design was traced with a grease pencil. By spreading a special substance on the wet plate, the drawn portion would hold it, while the color would not adhere to the rest of the stone. Drawing with a grease pencil was easier than producing a plate and allowed corrections. With this technique, the colors were printed first, and then the figures' outlines were traced in black. Since black has the highest covering power, this method hides any imperfections or smudges in the underlying colors. Thus, the colors appear well-aligned.

1.4 Modern Techniques

Lithography's tones are very flat, with colors lacking nuances or shading. To overcome this problem, the *chromolithography* technique was developed. This technique uses colored dots to create shadows or color gradients. The *photolithography* technique was developed in the second half of the 19th century. With this technique, printing is not done directly: the image is reproduced on a sheet of paper or a rubber plate, and then transferred to the final sheet. This system also allows a photograph to be used as a matrix. Finally, *dot lithography* uses colored dots obtained with halftones or electronically. However, not the entire image is screened, and the rest of the drawing uses solid colors.

2 Deck of Cards Under Reconstruction

While the English-style deck of cards is the most widely recognized international standard, many regions maintain distinct local decks that support the card games prevalent in their respective cultures [15,16,18].

These decks exhibit a high degree of standardization, as players seldom accept minor variations. In Italy, specifically, decks are often associated with individual regions. This regional diversity originated because, prior to 1861, Italy consisted of several independent states with distinct customs regulations, prompting each

state to develop its own local card designs. Within the former Papal States, the *Piacentine*-style deck of cards was prevalent, despite the fact that the city of Piacenza itself was geographically close but not part of the Papal States. In contrast, the classification of playing cards in the area surrounding Perugia (Umbria) remains more contentious. The following analysis examines a deck that, until the 1930 s, was identified as *Perugine*.

Guglielmo Murari was likely the most influential playing card manufacturer in Italy from the late nineteenth to the early twentieth century [10]. Born in Treviso, Veneto (then part of the Austrian Empire), in 1847, Murari was the son and grandson of established card manufacturers. The family relocated to Bari (Apulia) in 1867, where the business continued. In 1871, Guglielmo Murari assumed control of the enterprise. The Bari factory produced a significant volume of cards, manufacturing all local Italian patterns for distribution in regional markets. Among these products was the *Perugine* deck, which is illustrated in Fig. 2.



Fig. 2. *Perugine* cards produced by Murari (from Trinei's private collection).

During the second half of the nineteenth century in Perugia, the card manufacturer Verga was active. Verga produced large *Toscane* cards (see Fig. 3 (a)), small *Toscane* cards, and *Perugine* cards (see Fig. 3 (b)). The *Toscane* cards were likely intended for the nearby province of Arezzo in Tuscany, whereas the *Perugine* cards were certainly produced for local use. Subsequently, another Perugian manufacturer, Buoncompagni, produced large *Toscane* cards (see Fig. 3 (b)), while Bartolini manufactured *Perugine* cards (see Fig. 3 (c)). In the nearby city of Foligno in Umbria, Mariani also produced *Perugine*-type cards (see Fig. 4 (a)). Additionally, Mariani created a *Perugine*-type deck featuring a *Piacentine* ace of coins (see Fig. 4 (b)).

The Solesio family was among the most prominent card manufacturers. The Solesios originally produced playing cards in Spain and relocated to Genoa in the early nineteenth century. In the early twentieth century, the Solesio company manufactured *Perugine*-style decks of cards (see Fig. 5 (a)) and distributed them wrapped in sheets of paper engraved with "di tipo Perugia" (see Fig. 5 (b)).



(a) (b) (c)

Fig. 3. (a): large *Toscane* cards produced by Verga; (b): in the first row: small *Toscane* cards produced by Verga; in the second row: large *Toscane* cards produced by Buoncompagni; in the third row: *Perugine* cards produced by Verga; (c): *Perugine* cards produced by Bartolini [21].

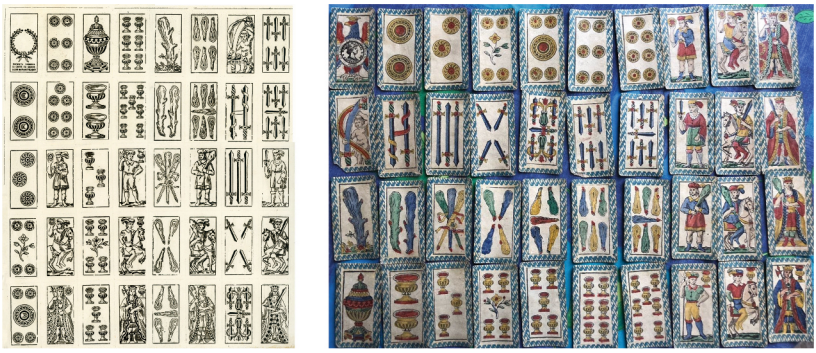

(a) (b)

Fig. 4. (a) and (b): *Perugine* cards produced by Mariani;



(a) (b)

Fig. 5. (a): *Perugine* cards produced by Solesio; (b): playing card wrapper by the Solesio company.

The *Perugine* type of cards has been discontinued since the 1930 s, making such decks extremely rare. This article examines a digital reconstruction of the Solesio deck with the objective of producing a new reprint, thereby enabling players in the Perugia area to reconnect with their gaming heritage.

3 The Direct Problem

In this section, we formalize the direct problem of image formation by xylographic techniques. Assume we have an ideal image composed of $u + 1$, with $u \geq 1$, subimages: one containing only the color black, and the other u containing a single, distinct color.

The black image contains only black and white pixels, while the colored images contain only pixels of a specific color or white. In these images, it is assumed that for each pixel, only at most one of the four subimages has a non-white pixel, except in the case of overlapping black and colored pixels in the internal regions of the image, where black does not correspond to the edge of an object. Furthermore, we assume that, in colored images, the colors completely cover connected regions of non-black pixels. Ideally, the black image contains the borders delimiting the colored areas with a nearly uniform thickness across the entire image, while other black objects depicting details can have different thicknesses.

During the printing phase, the resulting image ideally has a black pixel if it is black in the black image; otherwise, a colored pixel if it is colored with one of the three colors, or white if it is not colored in any of the four images. During this phase, due to xylographic printing, various alterations can occur. Due to wear and tear on the wooden printing press, the black image may exhibit alterations at the edges, where black pixels may be added or removed, replaced by new black, white, or intermediate-colored pixels. Note that the number of pixels added or removed at the edge varies, potentially altering the thickness of the black border. In some places, the black border may even be broken (see Fig. 6 (a) and (b)). This fact can be modeled using an appropriate probabilistic model, which must be determined on a case-by-case basis. The size of colored images may also vary at the edges due to printing; furthermore, some connected color areas may be slightly translated and rotated, resulting in imperfect overlap with the black border (see Fig. 6 (a)-(c)) and, in some areas, the overlapping of two colors. In the latter case, the resulting image will appear as a subtractive synthesis of the two overlapping colors.

Due to the temporal deterioration of the playing cards, there is a loss of saturation in all image components, including the white areas, as well as a slight blurring and the addition of noise, which we assume to be white and independent Gaussian. The blurring and loss of saturation may not be uniform across the image.

Finally, small color patches may be added to the image , whose colors depend on the area where they are inserted (see Fig. 6 (c)). This entire model presents many probabilistic variables and will be formalized and tested for validity in a subsequent work.



(a) (b) (c)

Fig. 6. (a): detail of the two of clubs, showing discontinuous black borders and red paint leakage beyond the borders; (b): detail of the ace of spades, illustrating discontinuous borders and an incomplete green area; (c): detail of the four of spades, indicating artificial color in some areas and an incomplete blue region. (Color figure online)

4 The Xylographic Image Reconstruction Problem

According to [13], the woodcut image reconstruction technique can be divided into five distinct phases. The first phase addresses damage resulting from paper and ink deterioration, which causes the data images to appear faded [1,9,19,20]. The defading technique proposed in [6] incorporates a deblurring step to reconstruct the diffusion of the paper ink. The second phase focuses on estimating the black border to separate various color regions. This task is classified as a curve reconstruction problem (see also [3,17]), and in [13], it is solved manually using established software tools. The third phase introduces a reconstruction process to remove artifacts and enhance color homogeneity, utilizing a regularization technique [7,8,11]. The fourth phase involves detecting the outer contour, which is distorted in the data due to the xylographic printing process and must therefore be estimated. To address this, an original regularization technique is employed, based on an energy function with three components: a coherence term to maintain proximity to the initial boundary, and two additional terms to regulate the boundary's length and thickness. The fifth and final phase estimates the intensity of undefined colors, using a variant of a classic sparse data resolution technique [14].

5 Segmentation Phase

This paper introduces a novel segmentation phase [12,22], positioned between the defading phase and the phase in which the black border of the image is reconstructed to address breaks generated during printing. This segmentation phase is essential, as it facilitates more direct management of subsequent processing steps. Furthermore, the xylographic reconstruction problem aligns more closely with a segmentation problem than with deblurring or regularization challenges. It is necessary to identify non-zero pixels in both the black and color images, as

well as to determine the specific color present in each color image. Consequently, the image must be segmented into $u + 1$ subimages.

To address the segmentation problem effectively, it is necessary to select a uniform color space in which adjacent colors appear similar to the human eye [4]. Specifically, we must group pixels with similar colors and assign them non-zero values. In this paper, the chosen color space aligns with that used in [13], namely the QTLC-r^*g^* (Quadratically Transformed Luminance Chrominance-r^*g^*) space, as introduced in [6]. This space is not only uniform but also supports the application of quadratic transforms when converting to the standard RGB space. The following subsection provides further details regarding this color space.

5.1 The QTLC-r^*g^* Color Space

Given a color $(r, g, b) \in [0, 255]^3$ in the RGB space, we initialy consider

$$\begin{cases} l = (1/4)r + (1/2)g + (1/4)b, \\ r^* = \dfrac{r-l}{l}, \qquad g^* = \dfrac{g-l}{l}. \end{cases}$$

l is the luminance coordinate of the color in the QTLC-r_*g_* space, the chrominance coordinates are computed as follows

$$\begin{cases} \alpha = (5/8)r^* - (3/8)g^* + (1/4)\, r^*\, g^* \\ \beta = (3/8)r^* + (5/8)g^*. \end{cases}$$

Given the image in Fig. 7 (a), Fig. 7 (b) presents its luminance; Fig. 7 (c) shows its chrominance; the component α and β are given in Fig. 7 (d), and (e), respectively.



(a) (b) (c) (d) (e)

Fig. 7. (a): king of coins of the *Piacentine* desk produced by Dal Negro; (b): the luminance component; (c): the chrominance component with constant luminance equal to 180; (d) the α component; (e) the β component.

To segment an image based on the colors used during the printing phase, it is necessary to analyze the chromatic components rather than the luminance.

Focusing on chrominance allows for the exclusion of variations in color intensity that are represented by luminance. Figure 8 shows a circular section of radius 1 of the chromatic components, with luminance set to a value of 180.



Fig. 8. chromatic space.

Let $t = \sqrt{(34+16\beta)^2 - 24(40\alpha + 24\beta)}$, then the inverse transforms from the QTLC-r^*g^* space into the RGB space is given by

$$\begin{cases} r = \frac{l}{12}(34 + 16\beta - t) + l, \\ g = \frac{l}{20}(-34 + 16\beta + t) + l, \\ b = 4l - r - 2g. \end{cases}$$

5.2 Proposed Techninique

Let image $X^{(1)} = (L^{(1)}, A^{(1)}, B^{(1)}) \in \mathbb{R}^{n\times m\times 3}$ be the faded image obtained after the first phase, where $L^{(1)}$ is the luminance component, and $A^{(1)}$ and $B^{(1)}$ the two components α and β, respectively.

We discretize the chromatic components on a grid with a fixed step h. Let $M(\alpha, \beta)$ be the number of occurrences of the chrominance component (α, β) in the image $X^{(1)}$. Now we divide the chrominance map into 4 areas associated with high-frequency chrominances, so that each area is almost connected. We do not require each map to be connected, as small chrominance bands may be randomly missing due to missing occurrences. We proceed as follows.

Since image $X^{(1)}$ is the result of a fading algorithm, its colors are highly saturated. We can assume that the maximum value of M occurs at $\alpha = \beta = 0$, where we have colors like black and white, and possibly some shades of gray.

We begin by creating a rectangular area on the map, centered at $\alpha = \beta = 0$, in which we will evaluate which high-frequency chrominances are connected to the chrominance $(0, 0)$. Note that we have to limit this area to a rectangle otherwise, we would find all the high-occurrence areas.

Consider the following procedure.

procedure Black
for $\alpha \in \{-2, 2\}$, with step h **do**
  for $\beta \in \{-2, 2\}$, with step h **do**

$f(\alpha,\beta)=0$;
end for
end for
for $\alpha \in \{\widetilde{\alpha},\overline{\alpha}\}$, with step h **do**
for $\beta \in \{\widetilde{\beta},\overline{\beta}\}$, with step h **do**
$f(\alpha,\beta)=1$;
end for
end for
$f(0,0)=2$;
for $\widetilde{h} \in \{-h,h\}$ **do**
for $\overline{h} \in \{-h,h\}$ **do**
for $\alpha \in \{\widetilde{\alpha},\overline{\alpha}\}$, with step $\widetilde{h}$ **do**
for $\beta \in \{\widetilde{\beta},\overline{\beta}\}$, with step $\overline{h}$ **do**
if $M(\alpha,\beta)>\varepsilon \wedge d(2,\alpha,\beta) \wedge f(\alpha,\beta)=1$ **then**
$f(\alpha,\beta)=2$;
end if
end for
end for
end for
end for
end procedure

By the first for loops, we impose that the partition to which all the color components belong is unknown, that is, $f(\alpha,\beta)=0$ for each pair (α,β). The second for loops imposes that the color components within a rectangle centered on the origin are selected, so $f(\alpha,\beta)=1$ for $(\alpha,\beta) \in [\widetilde{\alpha},\overline{\alpha}] \times [\widetilde{\beta},\overline{\beta}]$. The origin is inserted into the gray partition, so $f(0,0)=2$. In subsequent for loops, the rectangle centered on the origin is scanned four times in all possible directions, thus determining all the color components of the gray partition. If: the frequency of a particular component is high enough (i.e., $M(\alpha,\beta)>\varepsilon$, with ε an appropriate threshold); the distance between (α,β) and the gray partition is less than an appropriate threshold (in this case the value of the function $d(2,\alpha,\beta)$ is true); (α,β) is not yet part of the gray partition (i.e., $f(\alpha,\beta)=1$); then (α,β) is placed in the gray partition (i.e., $f(\alpha,\beta)=2$).

Now let's examine the following procedure.

procedure Chromatic Segmentation
for $k \in \{3,4,\ldots,u+2\}$; **do**
$(\hat{\alpha},\hat{\beta})=\arg\max_{f(\alpha,\beta)=0} M(\alpha,\beta)$;
$f(\hat{\alpha},\hat{\beta})=i$;
let $Q(l)$ be the occurrences of $(l,\hat{\alpha},\hat{\beta})$ in $X^{(1)}$;
$l^{(2)}(k)=\arg\max_{l\in[0,255]} Q(l)$;
$\alpha^{(2)}(k)=\hat{\alpha}$;
$\beta^{(2)}(k)=\hat{\beta}$;
for $\widetilde{h} \in \{-h,h\}$ **do**
for $\overline{h} \in \{-h,h\}$ **do**

```
      for α ∈ {α̃, ᾱ}, with step h̃ do
        for β ∈ {β̃, β̄}, with step h̄ do
          if M(α, β) > ε ∧ d(k, α, β) ∧ f(α, β) = 0 then
            f(α, β) = k;
          end if
        end for
      end for
    end for
  end for
end procedure
```

This procedure has u principal cycles, each of which determines a chromatic partition, denoted by $k \in \{3, 4, \ldots, u+2\}$. Initially, the maximizer $(\hat{\alpha}, \hat{\beta})$ of the occurrences of the components not yet assigned to any partition, i.e., such that $f(\alpha, \beta) = 0$, is determined. The component $(\hat{\alpha}, \hat{\beta})$ is thus assigned to the k-th partition, i.e., $f(\hat{\alpha}, \hat{\beta}) = k$. For each possible luminance l, the vector $Q(l)$ of the occurrences of $(l, \hat{\alpha}, \hat{\beta})$ in the image under consideration $X^{(1)}$ is determined. It is established that all pixels with a chromatic component belonging to the k-th partition will be assigned a luminance equal to the mode of the luminances of pixels with a chromatic component equal to $(\hat{\alpha}, \hat{\beta})$. Furthermore, all pixels of the partition under consideration will be assigned the chromatic component $(\hat{\alpha}, \hat{\beta})$. With successive for loops, the entire chromatic grid is scanned in all directions, and if: the frequency of a particular component is high enough (i.e. $M(\alpha, \beta) > \varepsilon$); the distance to the partition k is less than a suitable threshold ($d(k, \alpha, \beta)$ is true); (α, β) is not part of any partition ($f(\alpha, \beta) = 0$); then (α, β) is placed in partition k (i.e. $f(\alpha, \beta) = k$).

Finally, let's consider the main program.

```
main program
Black;
Chromatic Segmentation;
for i ∈ {1, ..., n} do
  for j ∈ {1, ..., m} do
    if f(α(i, j), β(i, j)) > 2 then
      α(i, j) = α^(2)(f(α(i, j), β(i, j)));
      β(i, j) = β^(2)(f(α(i, j), β(i, j)));
      l(i, j) = l^(2)(f(α(i, j), β(i, j)));
    end if
    if f(α(i, j), β(i, j)) = 2 then
      α(i, j) = 0;
      β(i, j) = 0;
      if l(i, j) < s then
        l(i, j) = 255;
      else
        l(i, j) = 0;
      end if
```

```
      end if
      if f(α(i,j),β(i,j)) = 1 then
        α(i,j) = 0;
        β(i,j) = 0;
        l(i,j) = 0;
      end if
      if f(α(i,j),β(i,j)) = 0 then
        l(i,j) = −1;
      end if
    end for
  end for
  while there exists (i,j) such that l(i,j) = −1 do
    for i ∈ {1,...,n} do
      for j ∈ {1,...,m} do
        if l(i,j) = −1 then
          update(l(i,j),α(i,j),β(i,j));
        end if
      end for
    end for
  end while
```

The main program begins by calling the two procedures, Black and Chromatic Segmentation. We have assumed that all variables in the two procedures are global and therefore visible in the main program. All pixels in the image $X^{(1)}$ are examined. If the partition assigned to the chromatic component of that pixel is a colored partition, i.e., $k \in \{3, 4, \ldots, u+2\}$, then the pixel's color components are assigned the values relative to the k-th partition. If the chromatic component of pixel (i, j) belongs to the gray partition, we proceed as follows: if the luminance exceeds a threshold s, the pixel is assigned the color white; otherwise, it is assigned the color black. We have decided to assign the color black to pixels whose chromatic components fall within the central rectangle but are not part of the gray partition (i.e., such that $f(\alpha(i,j),\beta(i,j)) = 1$). For pixels for which the chromatic component is indeterminate (i.e., $f(\alpha(i,j),\beta(i,j)) = 0$), we proceed as follows. We set the pixel value to indeterminate ($l(i,j) = -1$) and, as long as there are indeterminate pixels, we loop over them and update their value with the mode of the already determined pixels around them (function update$(l,(i,j),\alpha(i,j),\beta(i,j))$).

6 Experimental Results

The proposed technique was implemented in the C language on a Linux platform. Experimental results are reported for three different 1080×2000 data images. Because the original distortion-free images are not available, quantitative assessment of reconstruction quality is not feasible. Consequently, the quality of the results is evaluated visually. To this end, in this paper, the results of the proposed technique are compared with those obtained using the denoising technique

given in [8]. Our technique outcome serves as an intermediate step intended to enhance the quality of subsequent reconstructions, including automatic border closure and uniform coloring of enclosed areas.

Note that it is not possible to manually create the ideal original image, as this process would require arbitrary color selection. Consequently, any error measurement between the estimated image and the manually created image would primarily reflect differences in color choices rather than algorithmic performance. The proposed technique selects colors from the chromatic component of a uniform color space, which ensures more accurate and consistent color selection. In contrast, comparing the proposed technique with an alternative segmentation method is not feasible, as such a method would require significant simplification and adaptation to align with the specific requirements of the current problem. Additionally, fundamental differences in results would again arise from unpredictable color choices. Therefore, the proposed algorithm is compared with a regularization and denoising technique. The denoising method employed is sophisticated and incurs higher computational costs than the proposed approach; however, simpler denoising techniques may exist that achieve comparable results with reduced computational time. It is important to note that the output generated by the proposed algorithm serves as an intermediate step to facilitate

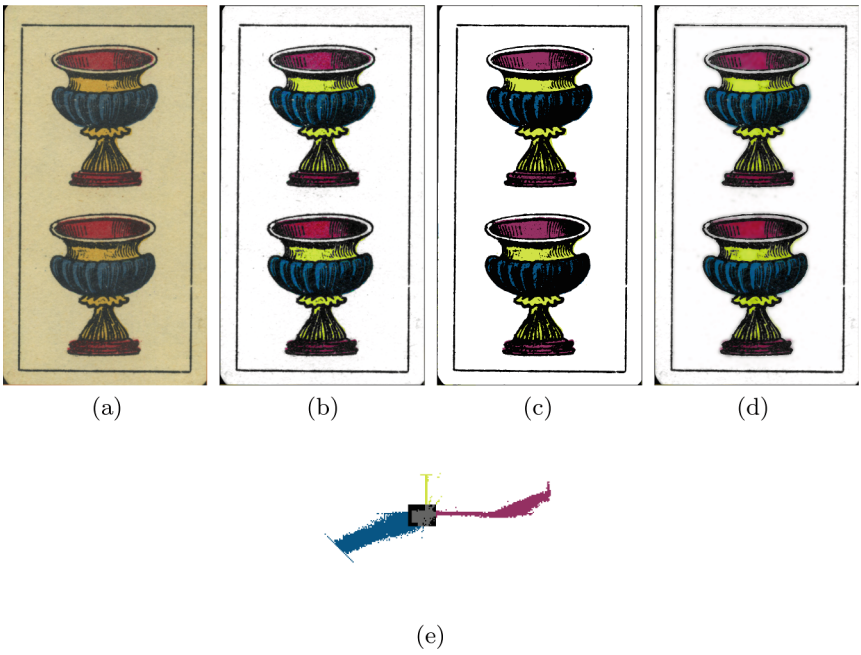

Fig. 9. (a): first data image; (b): defaded image; (c): segmented image; (d) denoised image; (e) segmented chrominance space.

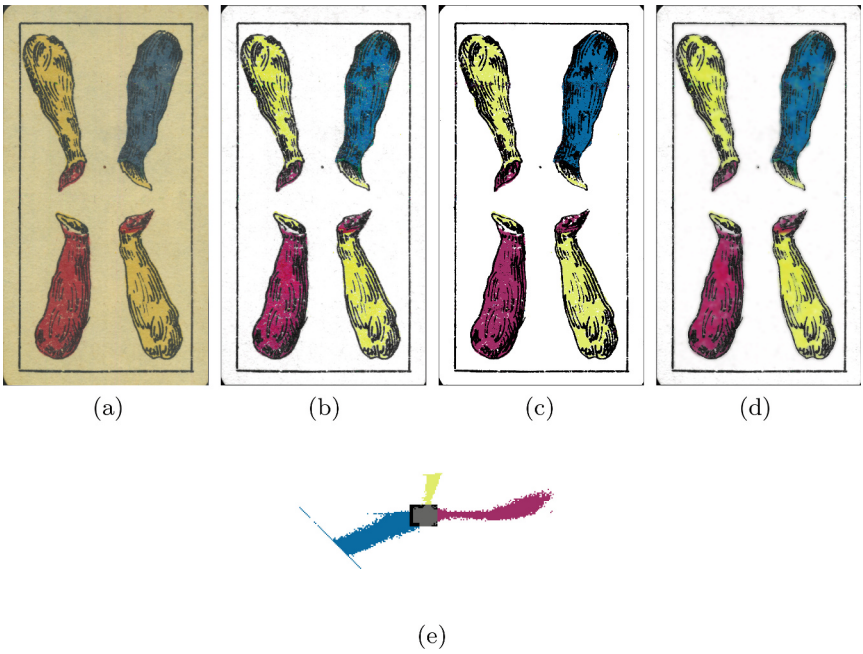

Fig. 10. (a): second data image; (b): defaded image; (c): segmented image; (d) denoised image; (e) segmented chrominance space.

the subsequent phase, which was previously performed manually and is currently under investigation.

The parameters utilized to evaluate the proposed algorithm are presented below. $h = 0.01$, $\widetilde{\alpha} = -0.15$, $\overline{\alpha} = 0.07$, $\widetilde{\beta} = -0.20$, $\overline{\beta} = 0.07$, $\varepsilon = 10$, and $s = 128$. These parameters were determined through experimental procedures.

Experimental results for the three images are shown in Figs. 9, 10, and 11. Each figure includes: (a) the data image to be processed; (b) the defaded data, denoted as $X^{(1)}$; (c) the output of the algorithm using three colors, denoted as $X^{(2)}$; (c) the reconstruction by the algorithm in [8]; and (d) the chromatic partition map given by the procedures Black and Chromatic Segmentation presented in the Subsect. 5.2. In the partition map, chromatic components classified as grey are shown in grey, components of the rectangle centered on the origin are shown in black, and colored components are displayed in their respective colors.

Figure 12 presents detailed views of the input images and the corresponding results produced by the proposed technique and the technique in [8]. In Figs. 12 (a), (d), and (e), the reconstructed image displays a completely white upper edge of the cup. In contrast, applying the denoising method yields a light gray edge. Examination of Figs. 12 (b), (e), and (f) shows that the green spots within the blue area are entirely removed, and the blue region remains unchanged. Note that the small details that remain incorrect can be easily removed in subsequent

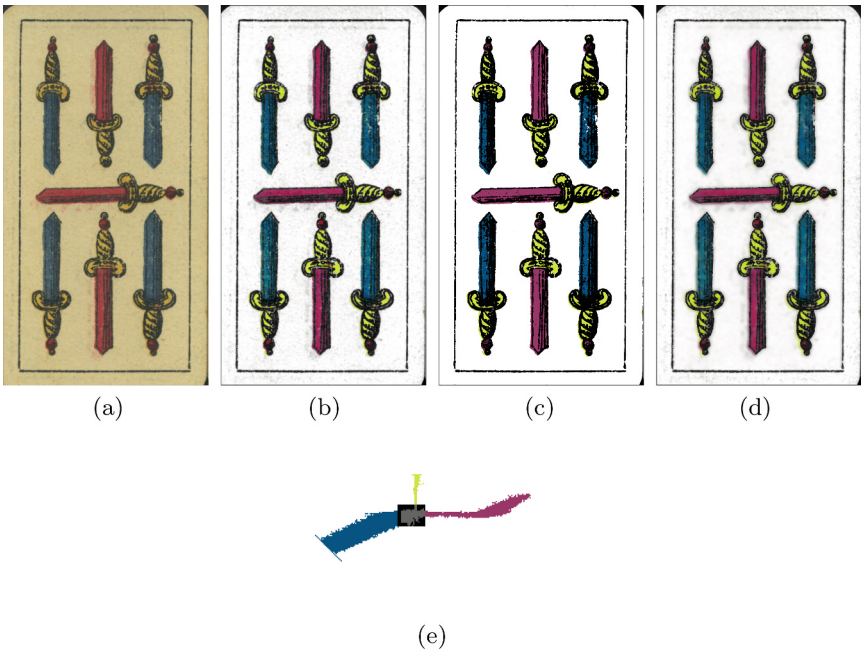

Fig. 11. (a): third data image; (b): defaded image; (c): segmented image; (d) denoised image; (e) segmented chrominance space.

phases. The denoising technique, however, alters the color. Finally, Figs. 12 (c), (f), and (i) demonstrate that the proposed technique effectively eliminates halos present in the data to be reconstructed. This result differs from that of the proposed denoising.

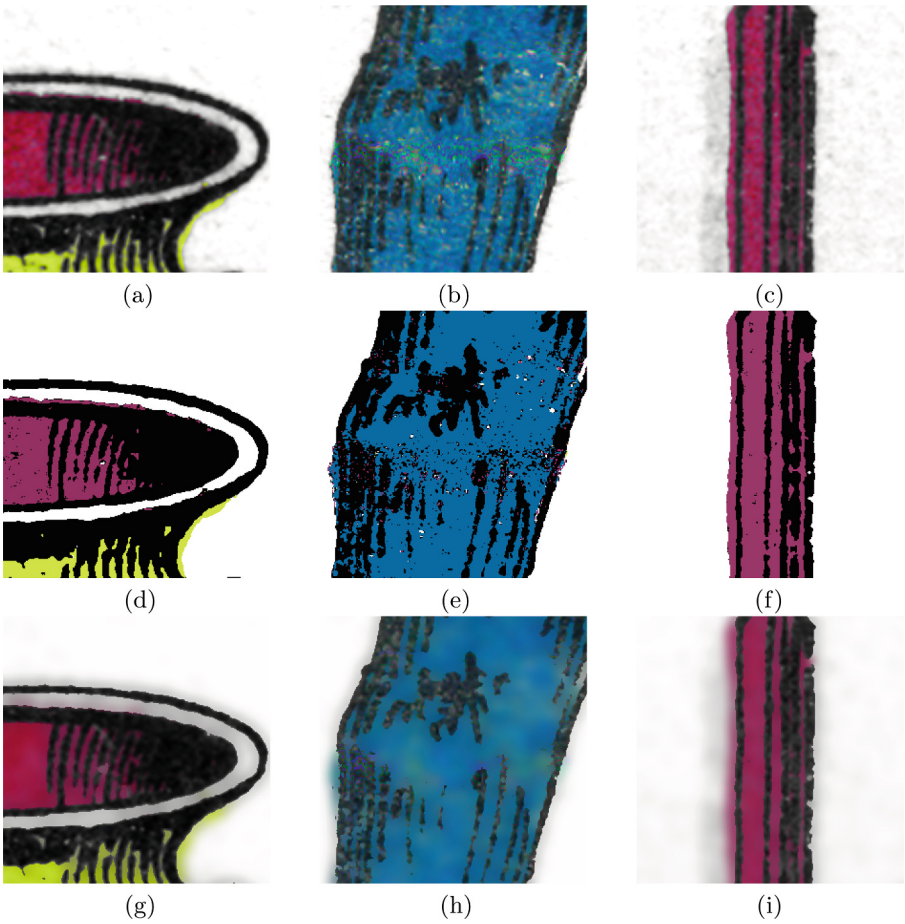

Fig. 12. (a): first defaded image detail; (b): second defaded image detail; (c): third defaded image detail; (d): first segmented image detail; (e): second segmented image detail; (f): third segmented image detail;(g): first denoised image detail; (h): second denoised image detail; (i): third denoised image detail.

Conclusions

This paper addresses the problem of reconstructing images of xylographic documents, noting that distortions in such images can manifest in various forms. Previous work [13] examined this issue in the context of reconstructing an ancient deck of *Perugine* playing cards, dividing the process into several phases. The present study introduces a new phase that segments pixels according to the printer's hues. Specifically, a technique based on the segmentation of the chromatic components within the uniform color space QTLC-r^*g^* (see [6]) is proposed. The experimental results are promising, particularly regarding their

application in subsequent reconstruction phases. A potential extension of this research involves evaluating all cards in the deck collectively to determine the overall print hues of the deck.

References

1. Ahmed, A. M. T.: Color restoration techniques for faded colors of old photos, printings, and paintings. In: Proceedings of 2009 IEEE International Conference on Electro/Information Technology, pp. 151–156 (2009)
2. Associazione 7bello – Cartagiocofilia Italiana A.P.S. https://www.7bellonline.it/. Accessed 20 Mar 2025
3. Barzegar Khalilsaraei, S., Komar, A., Zheng, J., Augsdörfer, U.: InceptCurves: curve reconstruction using an inception network. Vis. Comput. **40**, 4805–4815 (2024)
4. Basova, O., et al.: Uniform color space with advanced hue linearity: PCS23-UCS. In: Schettini, R., Trémeau, A., Tominaga, S., Bianco, S., Buzzelli, M. (eds) Computational Color Imaging. CCIW 2024. LNCS, vol 15193. Springer, Cham (2025)
5. Beal, G.: The printing of playing-cards. Playing-Card **29**(3), 106–114 (2000)
6. Biondi, G., Boccuto, A., Gerace, I.: Quadratically transformed luminance chrominance spaces. In: Gervasi, O., et al. Computational Science and Its Applications – ICCSA 2023 Workshops. ICCSA 2023. LNCS, vol. 14108. Springer, Cham. 676–693 (2023)
7. Boccuto, A., Gerace, I., Giorgetti, V.: A graduated non-convexity technique for dealing large point spread functions. Appl. Sci. **2** (10), 28 (2023)
8. Boccuto, A., Gerace, I., Martinelli, F.: Half-quadratic image restoration with a non-parallelism constraint. J. Math. Imaging Vision **59**(2), 270–295 (2017)
9. Bruni, V., Ramponi, G., Restrepo, A., Vitulano, D.: Context-based defading of archive photographs. EURASIP J. Image Video Process. **2009**(986183), 11 (2009)
10. De Giorgio N. A.: La manifattura delle carte da gioco di Guglielmo Murari. Comune di Veglie (2005)
11. Demoment, G.: Image reconstruction and restoration: overview of common estimation structures and problems. IEEE Trans. Acoust., Speech Signal Process. **37**, 2024–2036 (1989)
12. Erb, W.: Split-and-merge segmentation of biomedical images using graph wedgelet decompositions. In: Gervasi, O., et al. Computational Science and Its Applications – ICCSA 2025 Workshops. ICCSA 2025. LNCS, vol 15899. Springer, Cham. 252–263 (2025)
13. Gerace, I.: Digital reconstruction of ancient paper artifacts. In: Gervasi, O., et al. Computational Science and Its Applications – ICCSA 2025 Workshops. ICCSA 2025. LNCS, vol 15892. Springer, Cham, pp. 400–416 (2025)
14. Gerace, I., Palomba, C., Tonazzini, A.: An inpainting technique based on regularization to remove bleed-through from ancient documents. In: Proceedings of the 2016 International Workshop on Computational Intelligence for Multimedia Understanding (IWCIM), Reggio Calabria, Italy, pp. 1–5 (2016)
15. Hargrave, C.P.: An History of Playing Cards. Courier Corporation, United States (2014)
16. Jilley, R.: A History of Playing cards. Studio Vista, London (1973)
17. Laville, B., Blanc-Féraud, L., Aubert, G.: A Γ-convergence result and an off-the-grid charge algorithm for curve reconstruction in inverse problems. J. Math. Imaging Vision **66**, 572–583 (2024)

18. Mann, S.: Collecting Playing Cards. Howard Baker Press (1966)
19. Nikitenko, D., Wirth, M., Trudel, K.: Applicability of white-balancing algorithms to restoring faded colour slides: an empirical evaluation. J. Multimed. **3**(5), 9–18 (2008)
20. Restrepo, A., Ramponi, G.: Filtering and luminance correction for aged photographs. In: Image Processing: Algorithms and Systems VI, Proceedings of SPIE, vol. 6812, pp. 26–31, San Jose, Calif, USA (2008)
21. Tarot-as-Tarocchi. https://www.tarot-as-tarocchi.com/files/piacentine-perugia--1-.jpg. Accessed 17 Mar 2025
22. Zaitoun, N.M., Aqe, M.J.: Survey on image segmentation techniques. Proc. Comput. Sci. **65**, 797–806 (2015)